J Mol Model (2019) 25: 245
https://doi.org/10.1007/s00894-019-4107-3

ORIGINAL PAPER

Stability conditions of armchair graphene nanoribbon bipolarons

Ana Virgínia Passos Abreu[1] · Luiz Antonio Ribeiro Junior[1] · Gesiel Gomes Silva[1] · Marcelo Lopes Pereira Junior[1] · Bernhard Georg Enders[2] · Antonio Luciano Almeida Fonseca[1] · Geraldo Magela e Silva[1]

Received: 1 February 2019 / Accepted: 26 June 2019 / Published online: 24 July 2019

Abstract

Graphene nanoribbons are 2D hexagonal lattices with semiconducting band gaps. Below a critical electric field strength, the charge transport in these materials is governed by the quasiparticle mechanism. The quasiparticles involved in the process, known as polarons and bipolarons, are self-interacting states between the system charges and local lattice distortions. To deeply understand the charge transport mechanism in graphene nanoribbons, the study of the stability conditions for quasiparticles in these materials is crucial and may guide new investigations to improve the efficiency for a next generation of graphene-based optoelectronic devices. Here, we use a two-dimensional version of the Su–Schrieffer–Heeger model to investigate the stability of bipolarons in armchair graphene nanoribbons (AGNRs). Our findings show how bipolaron stability is dependent on the strength of the electron–phonon interactions. Moreover, the results show that bipolarons are dynamically stable in AGNRs for electric field strengths lower than 3.0 mV/Å. Remarkably, the system's binding energy for a lattice containing a bipolaron is smaller than the formation energy of two isolated polarons, which suggests that bipolarons can be natural quasiparticle solutions in AGNRs.

Keywords Bipolarons · Tight-binding · Electron–phonon coupling · Graphene · Nanoribbons

Introduction

Graphene has attracted considerable interest in materials science and condensed matter physics since free-standing graphene was unexpectedly found [1, 2]. The discovery of its rich variety of electronic properties has to lead to a revolution in the development of new organic optoelectronic devices [3]. Armchair graphene nanoribbons [2, 4–7], in turn, are 2D lattices formed by laterally confined strips of graphene sheets that have a fundamental characteristic for these purposes, namely a finite bandgap [8–10]. In this sense, much effort has been made to reach a good cost-efficiency compromise in obtaining GNR-based devices.

In organic semiconductors, the charge carriers are composite structures formed by an excess of charge interacting with local lattice deformations [11]. Polarons are the most common charge carriers in these systems [12–19]. Recently, the stability and transport of polarons in AGNRs were theoretically investigated in the framework of Su–Schrieffer–Heeger model [20]. However, studies involving the presence of other carrier species in AGNRs need to be addressed.

Some experimental and theoretical studies have investigated the underlying properties associated with the coexistence of polarons and bipolarons in organic semiconducting materials. Silva and coworkers have numerically studied the stability of polarons and bipolarons in conjugated polymers and concluded that bipolarons are more stable than polarons [21]. In such systems, the total energy is smaller with a bipolaron than with two isolated polarons. Moreover, it was found that critical electrical field to dissociate a bipolaron is an order of magnitude higher than for a polaron. Wang showed that the creation of a bipolaron could be energetically favorable in these systems, in the process of doping or photoexcitation [22].

In another work, Onodera and Okuno obtained analytical solutions to a *cis*-polyacetylene chain [16]. They showed that the energy levels inside the band gap are closer in

This paper belongs to the Topical Collection VII Symposium on Electronic Structure and Molecular Dynamics – VII SeedMol

✉ Geraldo Magela e Silva
magela@fis.unb.br

[1] Institute of Physics, University of Brasília, 70.919-970, Brasília, Brazil

[2] University of Brasília, PPG-CIMA, Campus Planaltina, 73345-010, Brasília, DF, Brazil

the case of bipolaron compared to the polaron. Besides, they also showed that the bipolaron formation, as a bonded polaron pair, is favorable because the formation energy for a bipolaron is smaller than an isolated polaron pair. At the same time, Bredas and Street showed the arrangement of energy levels inside the band gap of organic semiconductors with polaron and bipolaron [18]. They defined bipolaron as a bound pair of quasiparticles with the same charge, associated with a substantial deformation of the lattice. The energy gain with the lattice interaction in the bipolaron formation is more significant than Coulomb interaction between charges confined in the same region of the chain. They also showed that the bipolaron is more thermodynamically stable than two isolated polarons. Recently, Dhanker revealed via charge modulation spectroscopy that bipolarons concentration on the interface between electrodes and organic semiconductors is more significant than was previously believed [23]. Meng showed that in light-emitting diodes, the effect of promoting bipolaron recombination and the subsequent generation of bipolaron-excitons is dominant electroluminescence of polymers [24]. Importantly, these studies revealed the importance of bipolarons in one-dimensional organic materials. Therefore, from the findings of the works presented above, it is reasonable to infer that bipolarons can also be stable carrier structures in AGNRs.

Here, we study the stability of bipolarons in AGNRs. To do so, we use a modified tight-binding 2D model including lattice relaxation. Initially, we compare the charge localization for a bipolaron in a particular AGNR for different values of the electron-phonon coupling (e-ph) constant. After this, we evaluate the changes in the bipolaron band gap with the increment of the coupling constant. Finally, we investigate the relation between the coupling constant and the system's binding energy.

Methodology

Our two-dimensional tight-binding approach is based on a modified version of the of the Su–Schrieffer–Heeger (SSH) Hamiltonian [25, 26]. More details about our approach can be found in our recent works [27, 28]. The model Hamiltonian used here is given by $H = H_{\text{latt}} + H_{\text{elec}}$, where the first and second terms are denoting the lattice and electronic degrees of freedom, respectively. The lattice Hamiltonian—that is treated classically by employing a harmonic approximation [26]—assume the following form

$$H_{\text{latt}} = \frac{1}{2}\sum_{i}\frac{P_i^2}{M} + \frac{1}{2}\sum_{\langle i,j\rangle} K\eta_{i,j}^2, \tag{1}$$

where P_i is the momentum of the i-th site with mass M, and K is the force constant associated with the σ bond [26]. In the equation above, indexes i and j denote two arbitrary neighboring sites in the lattice (Fig. 1).

The electronic Hamiltonian, in turn, considers the π-electrons dynamics as described by the equation below,

$$H_{\text{elec}} = -\sum_{\langle i,j\rangle,s} t_{i,j}\left\{e^{-i\gamma\mathbf{A}\cdot\hat{r}_{i,j}}C_{i,s}^{\dagger}C_{j,s} + e^{i\gamma\mathbf{A}\cdot\hat{r}_{i,j}}C_{j,s}^{\dagger}C_{i,s}\right\}. \tag{2}$$

The summation runs over π-electrons in neighboring i and j sites with spin s. $C_{i,s}^{\dagger}$ and $C_{i,s}$ stand the creation and annihilation of an electron in states denoted by their subscript indices. $\gamma \equiv ea/\hbar c$, where a is the lattice parameter, e the fundamental charge, and c the speed of light. To consider an external electric field ($\mathbf{E}$), we use a vector potential according to

$$\mathbf{E}(t) = -\frac{1}{c}\mathbf{A}(t).$$

Still in Eq. 2, $t_{i,j}$ is the hopping integral that couples the π-electrons to the lattice and is described by the following

$$t_{i,j} = t_0 - \alpha\eta_{i,j}. \tag{3}$$

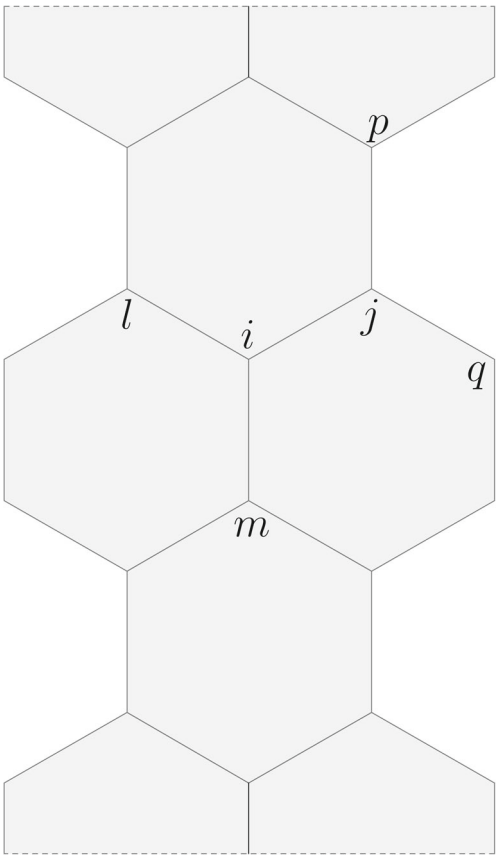

Fig. 1 Schematic representation of an armchair GNR. The site labeled as i has tree neighbors: j, l, and m

In Eq. 3 above, α is the electron-phonon coupling constant and $\eta_{i,j}$ is the relative displacement of the lattice sites from their equilibrium positions.

The interdependence between charge and lattice is considered by means of the electron–phonon coupling constant that introduces relaxation effects. The displacements of the carbon atoms are considerably small, which leads to the harmonic approximation for the σ-bonds. This same argument can be used to justify the first-order expansion in the hopping integral associated with π-electrons.

The initial system configuration contains a bipolaron in its ground state configuration. To achieve such an initial arrangement, we use the self-consistent procedure described in reference [27] that was developed to generate polarons in AGNRs. In the present work, the numerical protocol consists of removing from the lattice two electrons with antiparallel spins to create a positive bipolaron.

To solve the system dynamics, the time evolution of the initial state for the lattice is treated within the scope of the Euler–Lagrange equation [27]. The time evolution of the electronic part, in turn, is solved by using the time-dependent Schrödinger equation. In this way, the wave function $\psi_{k,s}(t)$ is expanded in the basis of eigenstates of the electronic Hamiltonian, $\phi_{l,s}(t)$, at a given time t so that the wave function in time $t + dt$ can be expressed as

$$\psi_{k,s}(i, t + dt) = \sum_{l,m} \phi_{l,s}(m, t)\psi_{k,s}(m, t)e^{-\frac{\epsilon_l(t)}{\hbar}dt}\phi_{l,s}(i, t), \tag{4}$$

where $\epsilon_l(t)$ is the eigenenergy of $\phi_{l,s}(t)$.

The solution of the Euler–Lagrange equation leads to the following Newtonian-type expression

$$M\ddot{\eta}_{i,j} = \frac{1}{2}K\left\{y\eta_{i,l} + \eta_{m,i} + \eta_{j,p} + \eta_{q,j} - 4B_{i,j}\right\} + \frac{1}{2}\alpha\left\{B_{i,l} + B_{m,i} + B_{j,p} + B_{q,j} - 4B_{i,j} + \text{c.c.}\right\}, \tag{5}$$

where

$$B_{i,j} = \sum_{k,s}{}' e^{-i\gamma\mathbf{A}\cdot\hat{r}_{i,j}}\psi^*_{k,s}(i, t)\psi_{k,s}(j, t). \tag{6}$$

$B_{i,j}$ couples the electronic and lattice degrees of freedom. The primed sum means that only the occupied states are considered. Importantly, to avoid edge effects we adopt periodic boundary conditions in the vertical direction of the nanoribbon, where the electric field is applied. The approach described above has been successfully used to study the polarons properties in AGNRs showing a good track record [29–31].

Results

The focus of this work is to investigate the dependence of the bipolaron stability in AGNRs as a function of the strength of the e-ph coupling constant. An expected result is the maintenance of the bipolaron stability for lower values of the e-ph coupling constant in according to what is observed when a polaron is simulated in the same system. In this sense, we considered, in our simulations, the coupling constant α—according the notation in references [27, 28]—ranging from 2.0 to 6.0 eV/Å, with an increment of 0.5 eV/Å, as depicted in Fig. 2. In this figure, we can assess how the charge localization pattern on the nanoribbon changes when the e-ph coupling constant varies. In this sense, one can note that the characteristic charge localization of a bipolaron increases when the strength of the coupling constant is increased. These results suggest a bipolaron stability improvement with the coupling constant increment. In previous work, a similar result was obtained while investigating the interplay between the e-ph coupling constant strength and the charge localization of a polaron in AGNRs [32]. The gain in the stability for the bipolaron can be observed by its integrity and localization for lower values of the coupling constant, as shown in Fig. 2. Only for $\alpha = 2.0$ eV/Å there is no characteristic charge localization of an quasiparticle, i.e., the charge is delocalized by all extension of the nanoribbon.

We now discuss the bond-length pattern presented by the lattice when a bipolaron is formed. To do so, Fig. 3 illustrates bond-length pattern for the cases depicted in Fig. 2. It is evident in this figure that the bond-lengths suffer higher deviations in the regions of the lattice containing a charge. When the charge localization increases, the bond-length distortion also increases. This mechanism is governed by the strength of the e-ph coupling parameter.

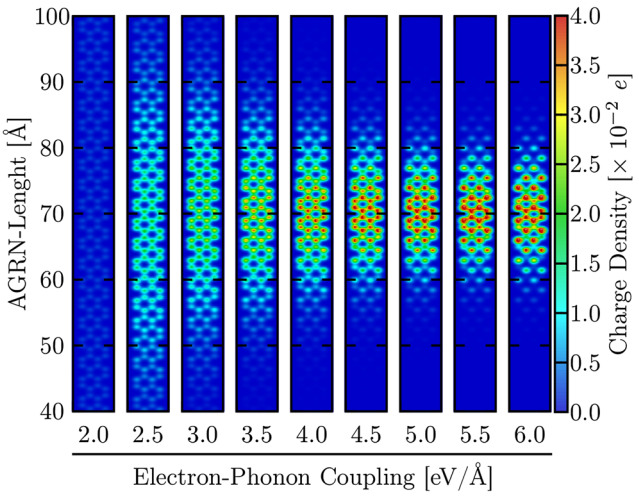

Fig. 2 Schematic representation of the charge localization of a 4x200 AGNR with a bipolaron

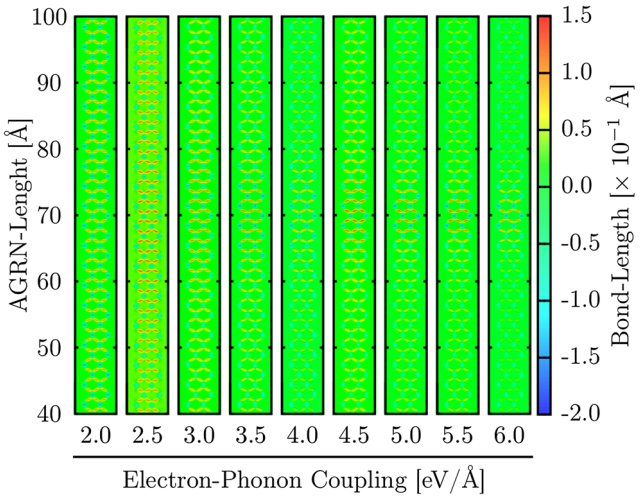

Fig. 3 Schematic representation of the bond lengths of a 4x200 AGNR with a bipolaron

Other evidence that bipolarons are quasiparticle species more stable than polarons is the localization signature presented by the energy levels inside the band gap. For the bipolaron case, the highest occupied molecular orbital (HOMO) and the lowest unoccupied molecular orbital (LUMO) levels are closer to each other and, consequently, they are more deepened inside the band gap. The behavior of the HOMO-LUMO gap as a function of the e-ph coupling strength, as shown in Fig. 4, suggests that the bipolaron stability enhances when the strength of the coupling constant increases. This result is evidenced by the decrease of the HOMO-LUMO difference with the increase of the coupling constant. Moreover, the trend presented in the interplay between HOMO-LUMO and e-ph coupling constant corroborates with the behavior exhibited by the charge localization pattern in the sense that higher charge localization directly implies in a gain of stability for the charge carrier.

We characterize the bipolaron stability by calculating the system's binding energy (BE). This measurement denotes the energy required to couple the charge and lattice, i.e., the amount of energy that is necessary to form stable quasiparticles. The BE can be defined as $BE = \epsilon_{BP} - 2\epsilon_P$, where ϵ_{BP} and ϵ_P are the bipolaron and polaron formation energies, respectively. The formation energy of a quasiparticle represents the difference between the energies for systems in the neutral ground state and a relaxed configuration in the presence of charge [33]. In this sense, $BE < 0$ denotes a parameter space in which the amount of energy necessary to form a stable bipolaron is smaller than the energy required to two polarons. In this case, bipolarons are possible solutions. On the other hand, $BE > 0$ denotes that the energetic solution is in the form of two isolated polarons. Based on this interpretation, Fig. 5 shows the calculated BE as a function of the e-ph coupling strength. The inset panel illustrates the polaron and bipolaron formations energies for the cases presented in Fig. 2. In Fig. 5, one can note that BE is smaller than 0 for all points, excluding the case for $\alpha = 2.0$ eV/Å, where BE is zero. Therefore, $\alpha = 2.5$ eV/Åis close to the threshold to form stable bipolarons. In other cases, self-consistent calculations always yield stable bipolarons as the solutions. In these cases, the local lattice deformations impose an energy barrier to the extra holes that are much higher than the electronic repulsion. As a consequence, the holes remain locally trapped and coupled to each other yielding a bipolaron.

Finally, we present the bipolaron dynamics in the presence of an external electric field. Figure 6 illustrates the time evolution for the bipolaron's mean charge density in an AGNR–4 with 200 Åof length with periodic boundary conditions for an electric field strength of 1.5 mV/Å, that is applied in the direction of the armchair length, and

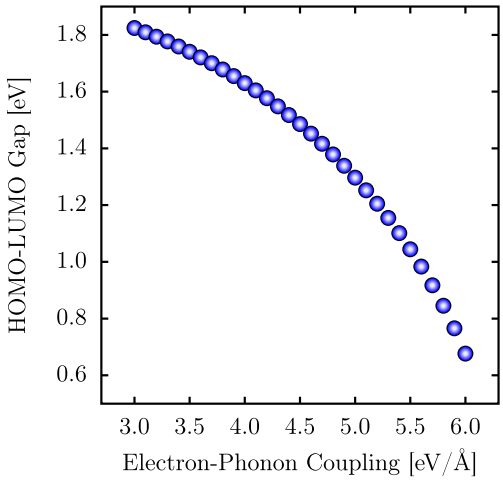

Fig. 4 Interplay between the HOMO-LUMO gap and the electron–phonon coupling strength

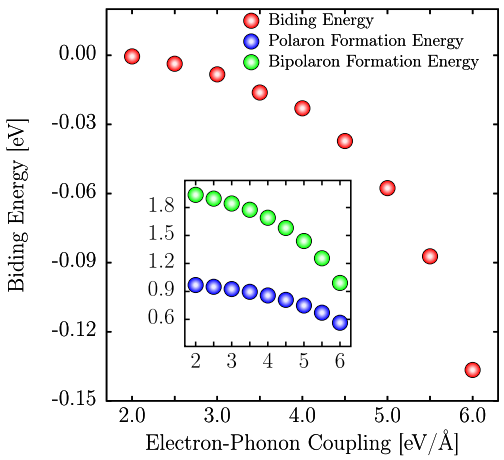

Fig. 5 System's binding energy as a function of the electron–phonon interactions

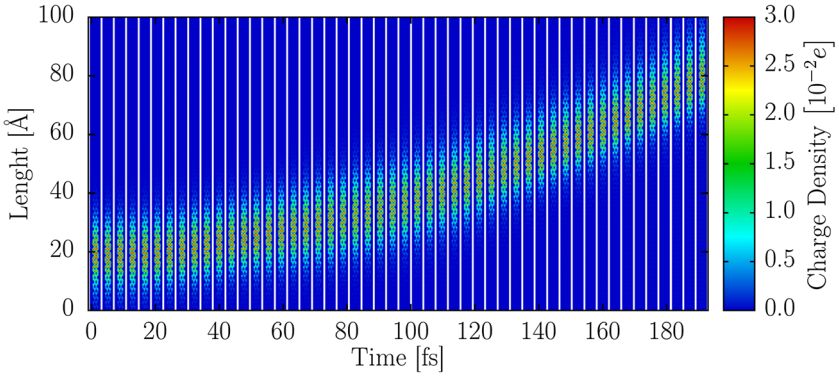

Fig. 6 Time evolution for the bipolaron's mean charge density in an AGNR–4 for an electric field strength of 1.5 mV/Å

e-ph coupling strength of 4.1 eV/Å. Each strip in this figure represents a different time step. In this sense, we note that the net charge presents a collective movement toward the direction of the applied field. Since the field strength is smoothly turned on up to the full value to avoid the bipolaron destabilization—according to the procedure presented in reference [34]—there is a delay in the bipolaron response to the applied electric field. After this transient time, the bipolaron reaches a steady-state moving linearly through the lattice. This trend of motion is evidenced by the changes in the vertical position of the net charge localization from left to right in the figure. The electric field also induces the charge localization that stabilizes the bipolaron during its motion. Importantly, the charge transport mechanism illustrated in Fig. 6 is evidence that the bipolarons are dynamically stable quasiparticles and may contribute with the charge transport mechanism in armchair graphene nanoribbons (AGNRs).

Conclusions

In summary, a two-dimensional tight-binding approach was employed to numerically study the impact of the electron–phonon interactions on the bipolaron properties in armchair graphene nanoribbons. Our findings showed that the bipolaron localization increases when the strength of e-ph coupling is increased. Moreover, it was obtained that the HOMO-LUMO difference decreases as the strength of the e-ph coupling constant increases. The system's binding energy calculated here suggests that bipolarons are quasiparticle present in AGNRs.

Acknowledgments The authors gratefully acknowledge the financial support from Brazilian Research Councils CNPq, CAPES, and FAPDF. This research work has the support of the Brazilian Ministry of Planning, Development and Management (Grants 005/2016 DIPLA – Planning and Management Directorate, and 11/2016 SEST – State-owned Federal Companies Secretariat) and the DPGU – Brazilian Union Public Defender (Grant 066/2016). L.A.R.J., B.G.E, and G.M.S gratefully acknowledge the financial support from FAPDF grants 0193.001511/2017, 0193.001.556/2017, and 0193.00176 6/2017, respectively. L.A.R.J. and G.M.S. gratefully acknowledge, respectively, the financial support from CNPq grants 302236/2018-0 and 304637/2018-1.

References

1. Geim AK, Novoselov KS (2007) Nat Mater 6:183. https://doi.org/10.1038/nmat1849
2. Miao F, Wijeratne S, Zhang Y, Coskun UC, Bao W, Lau CN (2007) Science 317(5844):1530. https://doi.org/10.1126/science.1144359. https://science.sciencemag.org/content/317/5844/1530
3. Dean CR, Young AF, Meric I, Lee C, Wang L, Sorgenfrei S, Watanabe K, Taniguchi T, Kim P, Shepard KL, Hone J (2010) Nat Nanotechnol 5:722. https://doi.org/10.1038/nnano.2010.172
4. Huertas-Hernando D, Guinea F, Brataas A (2009) Phys Rev Lett 103:146801. https://doi.org/10.1103/PhysRevLett.103.146801. https://link.aps.org/doi/10.1103/PhysRevLett.103.146801
5. Li X, Cai W, An J, Kim S, Nah J, Yang D, Piner R, Velamakanni A, Jung I, Tutuc E, Banerjee SK, Colombo L, Ruoff RS (2009) Science 324(5932):1312. https://doi.org/10.1126/science.1171245. https://science.sciencemag.org/content/324/5932/1312
6. Tan YW, Zhang Y, Bolotin K, Zhao Y, Adam S, Hwang EH, Das Sarma S, Stormer HL, Kim P (2007) Phys Rev Lett 99:246803. https://doi.org/10.1103/PhysRevLett.99.246803. https://link.aps.org/doi/10.1103/PhysRevLett.99.246803
7. Bolotin KI, Sikes KJ, Hone J, Stormer HL, Kim P (2008) Phys Rev Lett 101:096802. https://doi.org/10.1103/PhysRevLett.101.096802. https://link.aps.org/doi/10.1103/PhysRevLett.101.096802
8. de Oliveira Neto PH, Teixeira JF, da Cunha WF, Gargano R, e Silva GM (2012) J Phys Chem Lett 3(20):3039. https://doi.org/10.1021/jz301247u
9. Son YW, Cohen ML, Louie SG (2006) Phys Rev Lett 97:216803. https://doi.org/10.1103/PhysRevLett.97.216803. https://link.aps.org/doi/10.1103/PhysRevLett.97.216803
10. Ribeiro LA, da Cunha WF, Fonseca ALA, e Silva GM, Stafström S (2015) J Phys Chem Lett 6(3):510. https://doi.org/10.1021/jz502460g
11. Coropceanu V, Cornil J, da Silva Filho DA, Olivier Y, Silbey R, Brédas JL (2007) Chem Rev 107(4):926. https://doi.org/10.1021/cr050140x
12. Onodera Y (1984) Phys Rev B 30:775. https://doi.org/10.1103/PhysRevB.30.775. https://link.aps.org/doi/10.1103/PhysRevB.30.775
13. Brazoviskii SA, Kirova N (1981) JETP Lett 33:4
14. Boudreaux DS, Chance RR, Brédas JL, Silbey R (1983) Phys Rev B 28:6927. https://doi.org/10.1103/PhysRevB.28.6927. https://link.aps.org/doi/10.1103/PhysRevB.28.6927

15. Lin-Liu YR, Maki K (1980) Phys Rev B 22:5754. https://doi.org/10.1103/PhysRevB.22.5754. https://link.aps.org/doi/10.1103/PhysRevB.22.5754
16. Onodera Y, Okuno S (1983) J Physical Soc Japan 52(7):2478. https://doi.org/10.1143/JPSJ.52.2478
17. Stafström S, Chao KA (1984) Phys Rev B 30:2098. https://doi.org/10.1103/PhysRevB.30.2098. https://link.aps.org/doi/10.1103/PhysRevB.30.2098
18. Bredas JL, Street GB (1985) Acc Chem Res 18(10):309. https://doi.org/10.1021/ar00118a005
19. Kuhn C (1989) Phys Rev B 40:7776. https://doi.org/10.1103/PhysRevB.40.7776. https://link.aps.org/doi/10.1103/PhysRevB.40.7776
20. Silva GG, da Cunha WF, de Sousa Junior RT, Almeida Fonseca AL, Ribeiro Júnior LA, e Silva GM (2018) Phys Chem Chem Phys 20:16712. https://doi.org/10.1039/C8CP02373E
21. e Silva GM (2000) Phys Rev B 61:10777. https://doi.org/10.1103/PhysRevB.61.10777. https://link.aps.org/doi/10.1103/PhysRevB.61.10777
22. Wang CL, Su ZB, Martino F (1986) Phys Rev B 33:1512. https://doi.org/10.1103/PhysRevB.33.1512. https://link.aps.org/doi/10.1103/PhysRevB.33.1512
23. Dhanker R, Gray CL, Mukhopadhyay S, Nunez S, Cheng CY, Sokolov AN, Giebink NC (2017) Nat Commun 8(1):2252. https://doi.org/10.1038/s41467-017-02459-3
24. Di B, Meng Y, Wang YD, Liu XJ, An Z (2011) J Phys Chem B 115(30):9339. https://doi.org/10.1021/jp2006342
25. Su WP, Schrieffer JR, Heeger AJ (1979) Phys Rev Lett 42:1698. https://doi.org/10.1103/PhysRevLett.42.1698. https://link.aps.org/doi/10.1103/PhysRevLett.42.1698
26. Su WP, Schrieffer JR, Heeger AJ (1980) Phys Rev B 22:2099. https://doi.org/10.1103/PhysRevB.22.2099. https://link.aps.org/doi/10.1103/PhysRevB.22.2099
27. Ferreira da Cunha W, de Oliveira Neto PH, Terai A, e Silva GM (2016) Phys Rev B 94:014301. https://doi.org/10.1103/PhysRevB.94.014301
28. da Cunha WF, de Oliveira Neto PH, Ribeiro Junior LA, e Silva GM (2019) Phys Rev B 99:035405. https://doi.org/10.1103/PhysRevB.99.035405
29. da Cunha WF, Ribeiro LA, Fonseca ALA, Gargano R, e Silva GM (2015) Carbon 91:171. https://doi.org/10.1016/j.carbon.2015.04.065
30. Ribeiro LA, da Silva GG, de Sousa RT, Almeida Fonseca AL, da Cunha WF, e Silva GM (2018) Sci Report 8:1914. https://doi.org/10.1038/s41598-018-19893-y
31. Silva GG, da Cunha WF, de Sousa Junior RT, Fonseca ALA, Junior LAR, e Silva GM (2018) Phys Chem Chem Phys 20:16712. https://doi.org/10.1039/C8CP02373E
32. Abreu AVP, Teixeira JF, Fonseca ALA, Gargano R, e Silva GM, Ribeiro LA (2016) J Phys Chem A 120(27):4901. https://doi.org/10.1021/acs.jpca.5b12482
33. Stafström S (2010) Chem Soc Rev 39:2484. https://doi.org/10.1039/b909058b
34. Ribeiro LA, da Cunha WF, de Oliveria Neto PH, Gargano R, e Silva GM (2013) J New Chem 37:2829. https://doi.org/10.1039/C3NJ00602F